Hindawi Publishing Corporation
Journal of Nanomaterials
Volume 2015, Article ID 618492, 7 pages
http://dx.doi.org/10.1155/2015/618492

*Research Article*

# A Green and Facile Synthesis of Carbon-Incorporated $Co_3O_4$ Nanoparticles and Their Photocatalytic Activity for Hydrogen Evolution

**Libo Gao,[1,2] Jiangtao Diwu,[3] Qiang Zhang,[1,2] Hongyan Xu,[3] Xiujian Chou,[1,2] Jun Tang,[1,2] and Chenyang Xue[1,2]**

[1]*Key Laboratory of Instrumentation Science and Dynamic Measurement of Ministry of Education, North University of China, Taiyuan, Shanxi 030051, China*
[2]*Science and Technology on Electronic Test & Measurement Laboratory, North University of China, Taiyuan, Shanxi 030051, China*
[3]*School of Materials Science and Engineering, North University of China, Taiyuan, Shanxi 030051, China*

Correspondence should be addressed to Chenyang Xue; xuechenyang@foxmail.com

Received 15 June 2014; Revised 9 August 2014; Accepted 10 August 2014

Academic Editor: Shimou Chen



Carbon-incorporated $Co_3O_4$ nanoparticles with an average diameter of 50 nm were prepared via a facile and environmentally friendly one-pot carbon-assisted method using degreasing cotton as a template as well as a reactant. The elemental analysis indicates the incorporation of carbon species into the $Co_3O_4$ nanoparticles and the XPS measurements demonstrate the presence of carbon species which comes from the incomplete combustion of the degreasing cotton. Interestingly, the resultant sample was able to split pure water into hydrogen under visible light irradiation without any cocatalyst, which is mainly due to the enhanced light absorption behavior confirmed by the UV-Vis absorption spectra. This facile method provided a potential strategy for applying narrow bandgap semiconductors in pure water splitting.

## 1. Introduction

In recent years, photocatalytic production of hydrogen from water splitting has been regarded as an ideal solution to deal with the energy problem, due to its clean, nonprecious, and environmentally friendly production process via utilizing solar energy [1, 2]. In this field, a large amount of semiconducting materials have been explored to choose the ideal material which is capable of splitting water into hydrogen efficiently.

$Co_3O_4$ with a bandgap of 2.1 eV has been widely explored for photocatalytic production of $O_2$ from water splitting, owning to its excellent oxidation ability and low energy gap [3]. However, due to the lower conduction band minimum (CBM) compared to the $H^+$ reduction potential, much less reports on photocatalytic production of hydrogen have been reported. Although Zhang et al. reported that the $Co_3O_4$ quantum dots prepared by a reverse micelle method using a microwave-assisted solvothermal reaction had an excellent photocatalytic performance on splitting water into hydrogen because of the CBM upshift [4], this method required difficult procedures. Boumaza et al. reported that $Co_3O_4$, a multifunctional spinel-type p-type, was capable of promoting hydrogen photoproduction in the presence of methanol as sacrificial agent. This material, however, suffered rapid deactivation [5]. Therefore much research should go deep into the $Co_3O_4$ as a photocatalyst for hydrogen production.

It has been reported recently that carbon species can serve as sensitizers [6, 7]. Zhang et al. reported that the carbon species incorporated $TiO_2$ had a high hydrogen production rate, which is 1.8 times larger than that of P25, owning to the sensitization effect of carbon [8]. Kado et al. also synthesized $TiO_2$ with an enhanced photoresponse, which was modified by a thin carbon [9]. Nevertheless, $Co_3O_4$ modified with the carbon species as a photocatalyst for water splitting into hydrogen has not been reported.

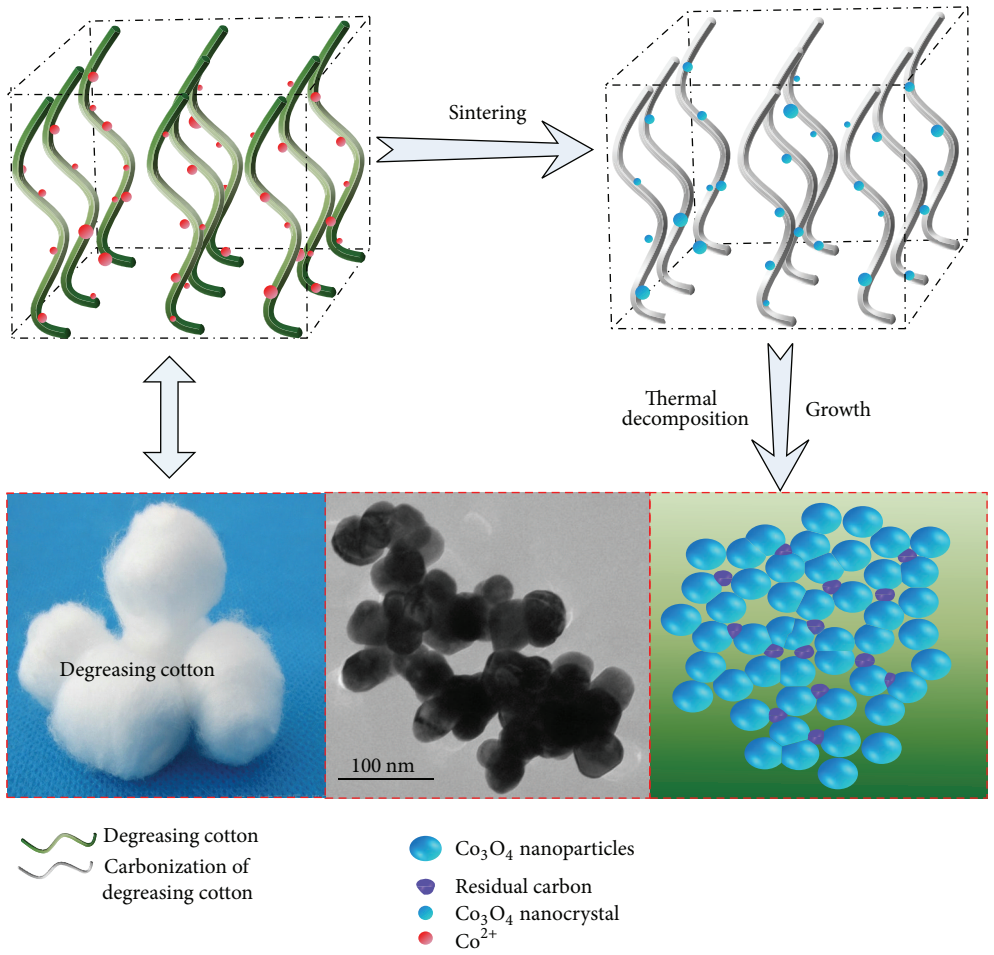


Scheme 1: Formation procedure of carbon-incorporated $Co_3O_4$.

In this work, a facile and environmentally friendly one-pot carbon-assisted method using degreasing cotton as a template as well as a reactant was used to synthesize the carbon-incorporated $Co_3O_4$ and its hydrogen production from photocatalytic splitting of water has been studied. To the best of our knowledge, this is the first time that the carbon-incorporated $Co_3O_4$ prepared as a photocatalyst was used to split water into hydrogen and the sample prepared interestingly even has photocatalytic activity under visible light irradiation.

## 2. Materials and Methods

*Synthesis*. Typically, 17.46 g $Co(NO_3)_2{\cdot}6H_2O$ was added to 20 mL deionized water followed by vigorous stirring for 10 min, producing a stable pink solution. Subsequently, 1.5 g degreasing cotton was immersed into the obtained pink solution and kept in an ultrasonic bath for 10 min in order to have a good dispersion of $Co^{2+}$ on the surface of degreasing cotton. Then the treated degreasing cotton was collected and transferred into a quartz petri dish in the tube furnace (OTF-1200X-III, Hefei, China) and kept at 600°C for 2 h in air. The resultant sample designated as $Co_3O_4$-DC was obtained without any postprocedures. For comparison, the product labeled as $Co_3O_4$-WA was fabricated directly calcining $Co(NO_3)_2$ solution at 600°C for 2 h without any additive.

The formation procedure is shown as Scheme 1.

*Characterization*. The crystal structure of the sample was performed through X-ray diffraction (XRD, a Bruker D8, $\lambda$ = 1.5406 Å) in the $2\theta$ of 10–80° with scan rate of 10°/min and Cu K$\alpha$ radiation, 40 KV. Scanning electron microscopy (SEM) images were obtained on a Hitachi S-4800 scanning electron microscope. The particle shapes and sizes were characterized by TEM measurement (JEOL JEM-1200EX) with a working voltage being 120 kv. Chemical composition analysis was carried out using energy dispersive X-ray (EDX) spectroscopy and X-ray photoelectron spectroscopy (XPS) which was collected using an ESCALAB 250Xi spectrometer with a standard Al K$\alpha$ radiation with the binding energies calibrated based on the contaminant carbon (C1s = 284.6 eV). The Raman spectrum was measured using a Renishaw inVia-Reflex Raman spectrometer. Specific surface areas and pore size distributions were computed from the results of $N_2$

physisorption at 77 K (Micromeritics ASAP 2020) by using the BET (Brunauer-Emmett-Teller) and BJH (Barrett-Joyner-Halenda). A Cary 300 Scan UV-Vis spectrophotometer was employed to record the UV-Vis diffuse reflectance spectra (DRS) in a region of 200 to 800 nm.

*Photocatalysis*. The photocatalytic activity for hydrogen production generated from water was estimated under simulated solar light condition. Typically, 0.02 g photocatalyst was added into the solution (~200 mL) containing 100 mL water and 100 mL ethanol as the sacrificial reagent, as it is more sustainable and renewable than methanol. The mixture was put in an ultrasonic stirring for 20 min, purged by Ar gas for 20 min, and then irradiated under simulated solar light with magnetic stirring. A 300 W Xe arc lamp (LSH-A500, Kaifeng Hxsei Science Instrument Co., Ltd., China) with UV cut-off filters (420 nm) was used as the light source. The hydrogen produced was analyzed by a gas chromatography (GC-9890B, Shanghai Linghua Instrument Co., Ltd., China) equipped with a thermal conductivity detector and a stainless steel column packed with molecular sieve (5A). Ar gas (99.999%) was used as the carrier gas.

## 3. Results and Discussions

*3.1. Characterization.* The XRD patterns of the $Co_3O_4$-DC are shown in Figure 1. No impurity peaks are found in the XRD patterns and all peaks have a good agreement with the standard spinel cubic $Co_3O_4$ spectrum (JCPDS number 42-1467; space group Fd-3m; lattice constant $a$ = 8.084 Å), suggesting that the sample produced is well-crystallized $Co_3O_4$ with high purity. The crystalline sizes of $Co_3O_4$-DC and $Co_3O_4$-WA (see the supporting information Figure S1 in the Supplementary Material available online at http://dx.doi.org/10.1155/2015/618492) calculated from the strongest peak located at (311) plan, respectively, are estimated to be 51.64 nm and ~100 nm according to Scherrer's formula, $D = 0.89\lambda/(B\cos\theta)$ ($D$, average dimension of crystallites; $\lambda$, the X-ray wavelength; $\theta$, the Bragg angle; $B$, the pure diffraction broadening of a peak at half-height), thus confirming that the crystal size of $Co_3O_4$-DC is much smaller than that of $Co_3O_4$-WA.

To further observe the morphologies of $Co_3O_4$-DC and $Co_3O_4$-WA, SEM and TEM were performed. It is clear from the panoramic view (insets (a), (b), and (c) of Figure 1) that the $Co_3O_4$-DC interestingly contains uniform and weak agglomerated $Co_3O_4$ nanospheres with 50 nm in diameter, which is in accordance with the value calculated from XRD. In addition, disordered hole-like arrangement of pores also can be seen in inset (a), making a promising favor to facilitate the water splitting due to the large specific surface area. The BET surface area and BJH pore size distributions of the as-prepared $Co_3O_4$-DC are shown in Figure S2 and the BET surface area is calculated to be 17.46 $m^2\,g^{-1}$ and the average pore size is 23.67 nm while the $Co_3O_4$-WA is only 5.8 $m^2\,g^{-1}$. Thus the $Co_3O_4$-DC should have more active sites in principle, which is beneficial to the photocatalytic splitting water into hydrogen [10]. Nevertheless, the $Co_3O_4$-WA

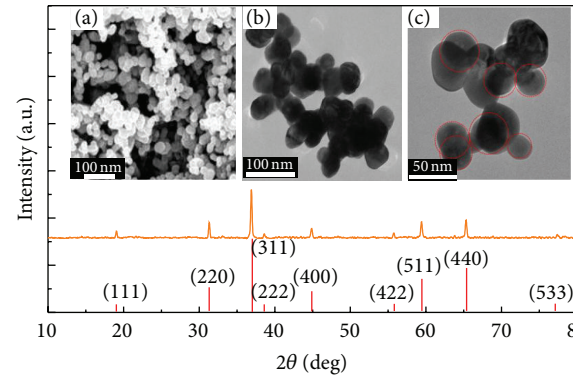


Figure 1: XRD patterns of $Co_3O_4$-DC and the inset is (a) SEM image; ((b), (c)) TEM images of $Co_3O_4$-DC. The inset bottom red bars indicate the standard reflections from $Co_3O_4$ (JCPDS number 42-1467).

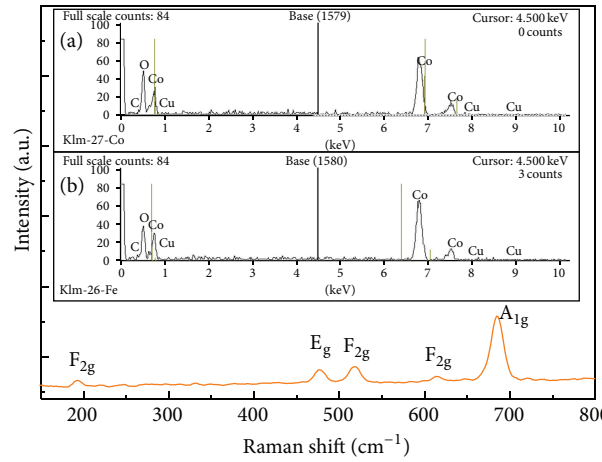


Figure 2: Raman spectrum of the $Co_3O_4$-DC. The insets are element analysis on the surface (a) and the cross section (b) of the $Co_3O_4$-DC.

nanoparticles despondingly have geometric irregular shapes which are spherical or rod-like structure with a particle size of ~100 nm, as shown in Figure S3.

Based on the analysis above, it is proved that the degreasing cotton used in the carbon-assisted method plays an important role in the fabrication of the $Co_3O_4$-DC with both regular morphology and high crystallization.

In an attempt to clarify the structure of the $Co_3O_4$-DC, Raman spectrum was performed due to its sensitivity on the microstructure of nanocrystalline materials. As shown in Figure 2, five obvious peaks are found at 192.4, 476.1, 518.3, 614.5, and 685.2 $cm^{-1}$, respectively, corresponding to the five Raman-active modes ($A_{1g}$, $E_g$, and $3F_{2g}$) of $Co_3O_4$. The Raman shifts are consistent with those of pure crystalline $Co_3O_4$ [11], revealing that the sample has a similar crystal structure to bulk $Co_3O_4$.

The insets of Figure 2 show the elemental analysis for the $Co_3O_4$-DC. The carbon content in the nanoparticles is 31.5 at% (atomic percent) on the surface (the inset (a) of Figure 2) and 24.35 at% in the cross section (inset (b) of Figure 2),

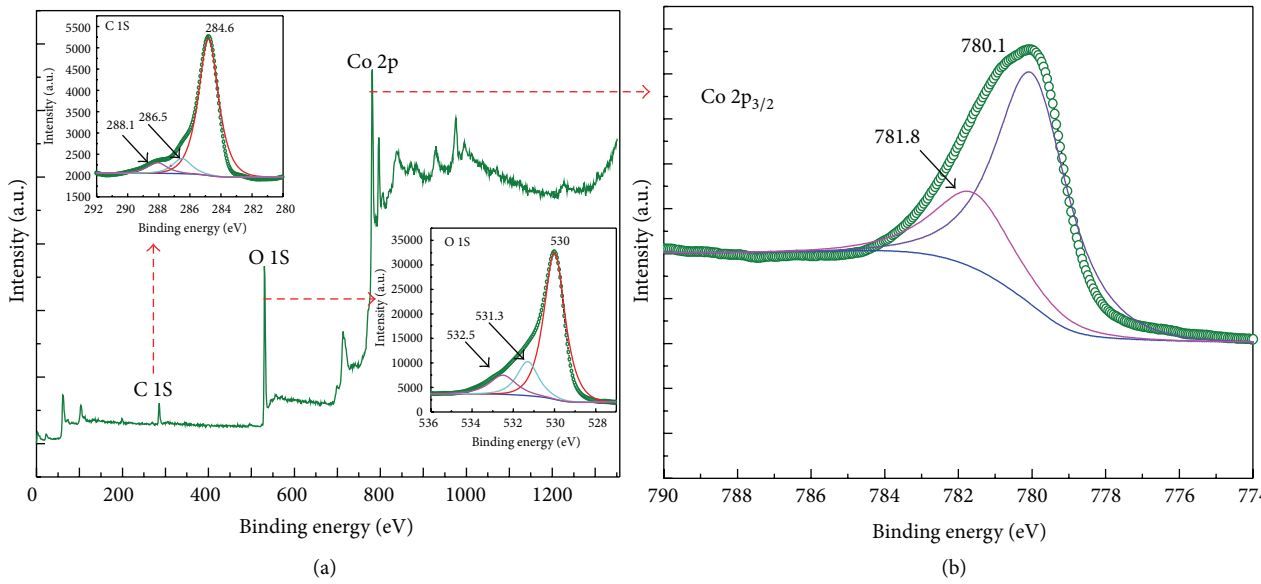


Figure 3: (a) XPS survey spectrum of the $Co_3O_4$-DC. The inset of (a) is the high resolution XPS C 1S and O 1S. (b) The high resolution XPS Co $2p_{3/2}$.

respectively. These results indicate the incorporation of carbon species into the $Co_3O_4$ nanoparticles, as a result of incomplete decomposition of degreasing cotton.

Figure 3 presents the X-ray photoemission spectroscopy (XPS) of $Co_3O_4$-DC to estimate the chemical composition of the sample. Peaks corresponding to cobalt, carbon, and oxygen are detected in the spectrum, indicating that only Co, O, and C elements can be found in the $Co_3O_4$-DC. The strong peak of C 1S centers at 284.6 eV can be assigned to elemental carbon which has given rise to the incomplete burning of degreasing cotton [12]. The other two weak peaks showed at 286.5 and 288.1 eV, respectively, which, as expected, are ascribed to the C–O bonds from insufficient combustion residual degreasing cotton [13, 14]. Additionally, no Co–C bond at 282.5 eV has been clearly found [15], revealing that nearly no carbon is doped into the lattice of $Co_3O_4$. As a consequence, it is proved that the carbon species incorporated in $Co_3O_4$ matrix are almost present as elemental state, which is in line with the results obtained in Teng's work [12].

The inset of Figure 3(a) shows the O 1S spectrum of the evaluated sample. The asymmetric O 1S spectra are fitted using two component peaks centered at 530 and 531.3 eV, which are ascribed to the surface lattice oxygen species and the surface adsorbed oxygen species ($O^{2-}$ or $O^{-}$), respectively [16]. The peak at 532.5 can be assigned to C–O [8], which is caused by the incomplete decomposition of degreasing cotton. Figure 3(b) gives the Co $2p_{3/2}$ high resolution XPS spectrum of the as-synthesized $Co_3O_4$-DC. The peaks at 780.1 and 781.8 eV correspond to $Co^{3+}$ and $Co^{2+}$, respectively [17, 18]. The ratio of $Co^{3+}/Co^{2+}$ on the surface of $Co_3O_4$-DC estimated by quantitative analysis is 2.84 instead of 2 in the chemical form of $Co^{2+}(Co^{3+})_2O_4$ while it is 1.89 in that of the $Co_3O_4$-WA (Figure S4), and the probable reason is the presence of abundant surface oxygen vacancies on the $Co_3O_4$-WA with much less defects on $Co_3O_4$-DC [16]. Importantly, it has been confirmed that less defects give rise to higher photocatalytic activity, as the recombination between photogenerated electrons and holes is decreased at the defect [19], thus indicating that our prepared sample may have a better performance on splitting water into hydrogen.

The optical absorption properties of the $Co_3O_4$-DC were investigated at room temperature by UV-Vis spectroscopy (Figure 4(a)). It is obvious that more intense and broad background absorption in the visible light region is observed for $Co_3O_4$-DC, and the absorption edges shift to longer wavelength compared with that of $Co_3O_4$-WA. The carbon residuals on the $Co_3O_4$-DC may be responsible for this phenomenon. In addition, the bandgap *Eg* value calculated according to the UV-Vis spectroscopy of $Co_3O_4$-DC is 2.0 eV (Figure 4(b)) which was greater than that of $Co_3O_4$-WA (*Eg* = 1.9 eV, inset of Figure 4(c)). The increase in the bandgap of the $Co_3O_4$-DC may be ascribed to the quantum confinement effects of nanomaterials [20]. Importantly, inset of Figure 4(a) shows the valence band maximum of $Co_3O_4$-DC and $Co_3O_4$-WA, clearly indicating that they have almost the same position of valence-band XPS spectra, thus demonstrating that bandgap widening of $Co_3O_4$-DC was mainly attributed to the conduction band minimum upshift, which would provide higher potential for $H^+$ reduction beneficial for photocatalytic hydrogen production.

Control experiments demonstrated that no hydrogen was evolved when the reaction proceeded without a photocatalyst or in the dark under stirring conditions while other conditions remained unchanged.

Figure 5(a) shows the photocatalytic hydrogen production on $Co_3O_4$-DC and $Co_3O_4$-WA at water/sacrificial agent (1 : 1) under simulated solar light. Higher photocatalytic splitting of water is observed for the $Co_3O_4$-DC (0.85 umol

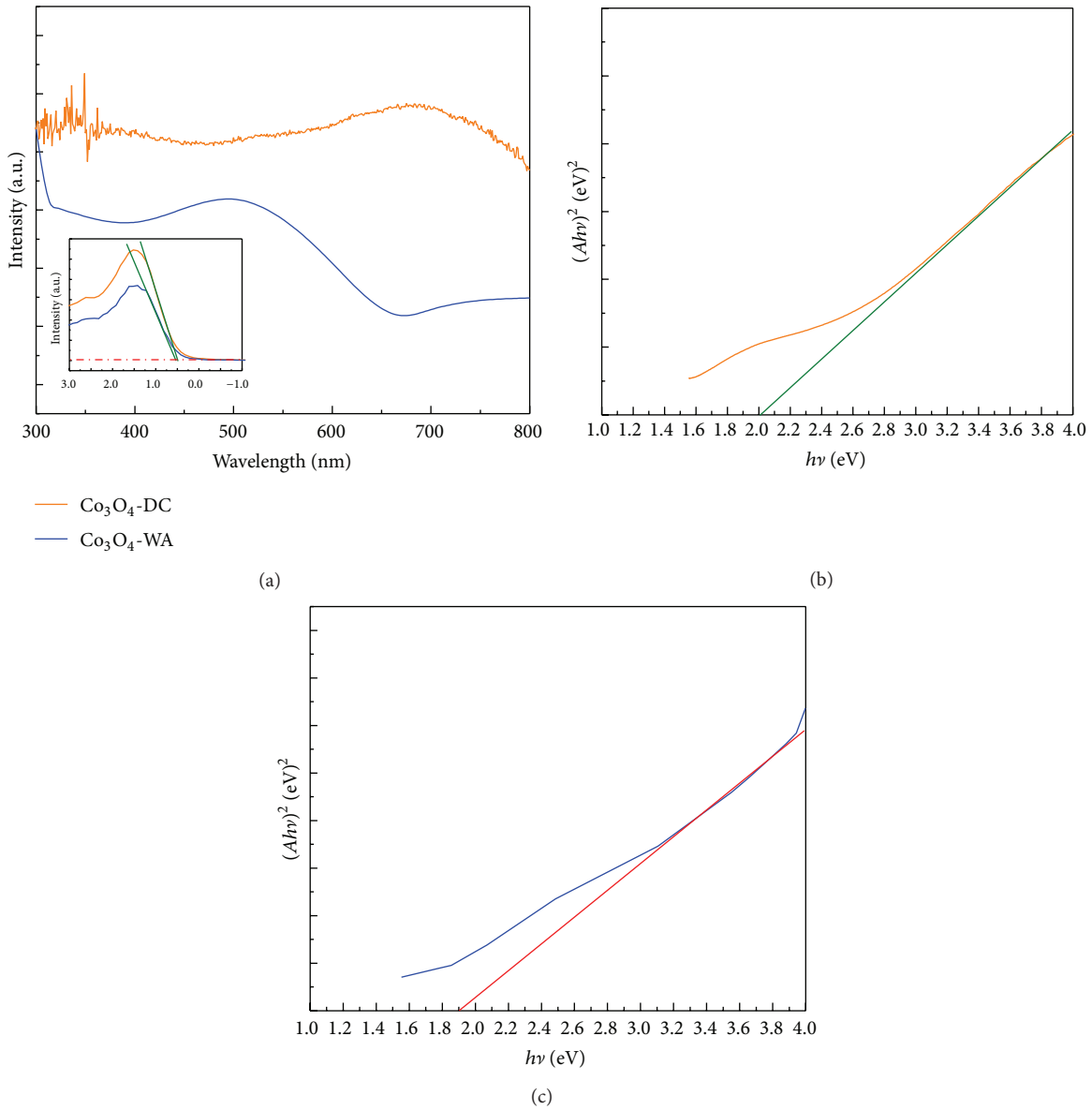


Figure 4: (a) UV-Vis spectrum of $Co_3O_4$-DC and $Co_3O_4$-WA, (b) $(Ahv)^2$-$hv$ curve of $Co_3O_4$-DC, and (c) $(Ahv)^2$-$hv$ curve of $Co_3O_4$-WA. Inset of (a): valence-band XPS spectra of $Co_3O_4$-DC and $Co_3O_4$-WA.

$h^{-1}$) as compared to that of $Co_3O_4$-WA (0.57 umol $h^{-1}$). The improvement of activity of $Co_3O_4$-DC could be ascribed to the small particle size and a high surface area resulted from the disordered hole-like arrangement of pores produced by the decomposition of degreasing cotton as a hard template, an abundance of oxygen vacancies, and a much more intense and broad background absorption in the visible light region which were caused by the sensitization of carbon residuals. Figure 5(b) displays the photocatalytic hydrogen production on $Co_3O_4$-DC and $Co_3O_4$-WA at pure water under simulated soar light; the hydrogen product decreases to 0.13 umol $h^{-1}$ for $Co_3O_4$-DC, indicating that the sacrificial agent has a significant effect on the photocatalytic hydrogen production. It is evidently seen that $Co_3O_4$-DC showed photocatalytic activity for hydrogen evolution while $Co_3O_4$-WA did not have a photocatalytic performance in pure water under visible light (Figure 5(c)). Zhang et al. [8] and Lettmann et al. [21] have proved that the carbon residuals in semiconducting metal oxide are prone to carrying out a charge transfer process and are responsible for the photosensitization of semiconducting metal oxide. Thus, the enhanced photocatalytic activity of the sample can be ascribed to the sensitization effect of carbon and the conduction band minimum upshift. Proposed mechanism for photocatalytic hydrogen production for $Co_3O_4$-DC is shown in Figure 5(d). After an electron is excited from the carbon residual by light irradiation, the electron is injected to the conduction band of $Co_3O_4$; meanwhile, the electron excited in $Co_3O_4$ also takes part in the hydrogen production and then hydrogen evolves on the surface of $Co_3O_4$ [22]. These results confirm that the carbon-incorporated $Co_3O_4$

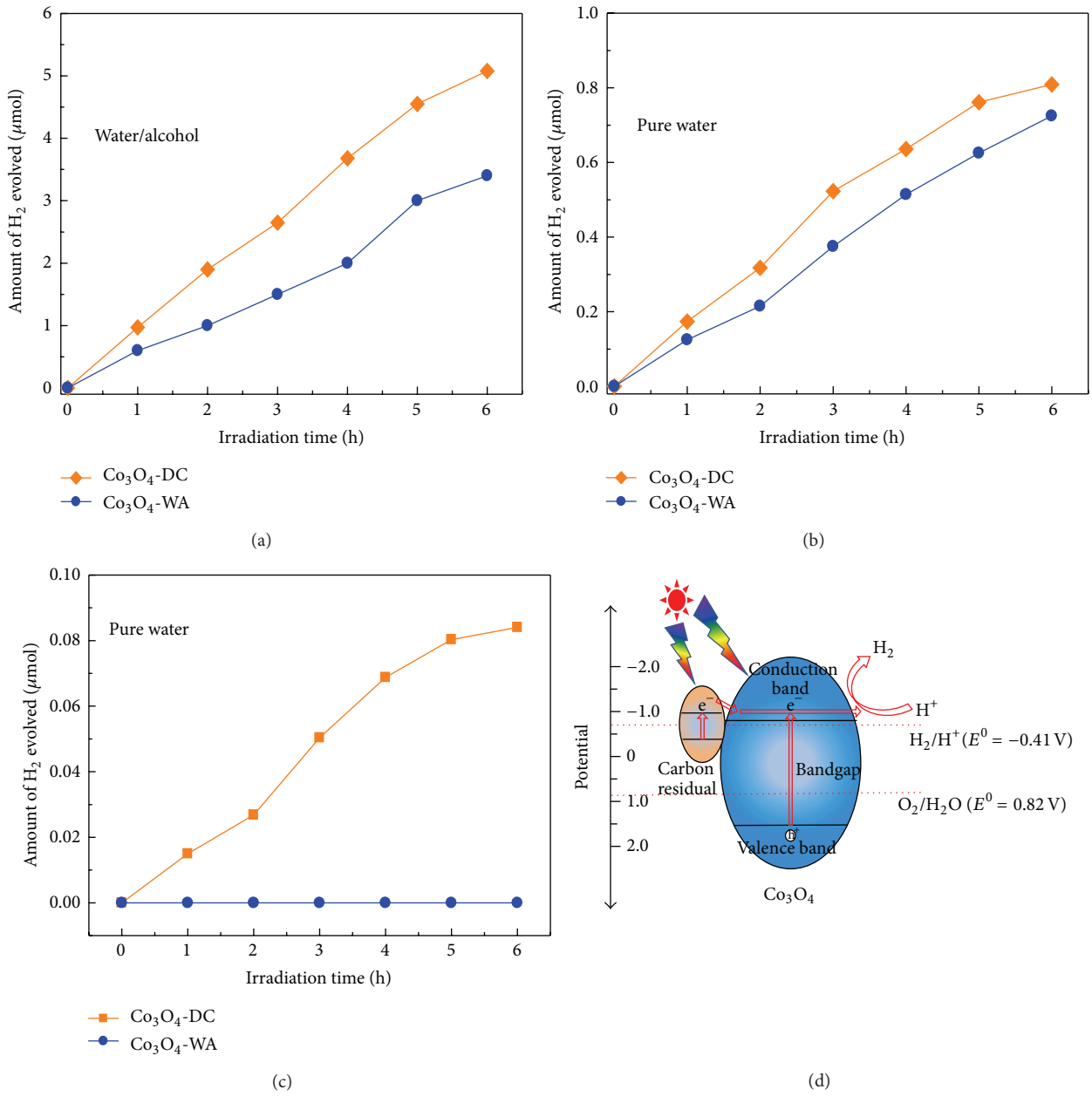


FIGURE 5: Photocatalytic hydrogen production on $Co_3O_4$-DC and $Co_3O_4$-WA under simulated solar light at (a) water/sacrificial agent (1 : 1); (b) pure water; (c) photocatalytic hydrogen production on $Co_3O_4$-DC and $Co_3O_4$-WA under visible light at pure water; (d) proposed mechanism for photocatalytic hydrogen production for $Co_3O_4$-DC at pure water.

synthesized via carbon-assisted method using degreasing cotton has a good performance in hydrogen production and even has photocatalytic ability under visible light for hydrogen evolution.

## 4. Conclusions

In summary, carbon-incorporated $Co_3O_4$ was successfully prepared by a facile and environmentally friendly carbon-assisted method using degreasing cotton and further applied as a photocatalyst in photocatalytic water splitting for hydrogen evolution. The carbon-incorporated $Co_3O_4$ was able to split pure water into hydrogen under visible light condition without any cocatalyst, which is mainly due to the sensitization effect of carbon. In addition, it provided a potential strategy for applying narrow bandgap semiconductors in pure water splitting.

## Conflict of Interests

The authors declare that there is no conflict of interests regarding the publication of this paper.

## Acknowledgments

The authors gratefully acknowledge the support of this research by the National Natural Science Foundation of China (no. 91123616 and no. 51105345). They also deeply appreciate the referee's valuable comments, which have greatly enhanced the quality of the paper.

## References

[1] X. B. Chen, S. H. Shen, L. J. Guo, and S. S. Mao, "Semiconductor-based photocatalytic hydrogen generation," *Chemical Reviews*, vol. 110, no. 11, pp. 6503–6570, 2010.

[2] R. Abe, "Recent progress on photocatalytic and photoelectrochemical water splitting under visible light irradiation," *Journal of Photochemistry and Photobiology C: Photochemistry Reviews*, vol. 11, no. 4, pp. 179–209, 2010.

[3] S. Yusuf and F. Jiao, "Effect of the support on the photocatalytic water oxidation activity of cobalt oxide nanoclusters," *ACS Catalysis*, vol. 2, no. 12, pp. 2753–2760, 2012.

[4] N. Zhang, J. Shi, S. S. Mao, and L. Guo, "$Co_3O_4$ quantum dots: reverse micelle synthesis and visible-light-driven photocatalytic overall water splitting," *Chemical Communications*, vol. 50, no. 16, pp. 2002–2004, 2014.

[5] S. Boumaza, R. Bouarab, M. Trari, and A. Bouguelia, "Hydrogen photo-evolution over the spinel $CuCr_2O_4$," *Energy Conversion and Management*, vol. 50, no. 1, pp. 62–68, 2009.

[6] C. Chen, M. Long, H. Zeng et al., "Preparation, characterization and visible-light activity of carbon modified $TiO_2$ with two kinds of carbonaceous species," *Journal of Molecular Catalysis A: Chemical*, vol. 314, no. 1-2, pp. 35–41, 2009.

[7] J. Zhong, F. Chen, and J. Zhang, "Carbon-deposited $TiO_2$: synthesis, characterization, and visible photocatalytic performance," *Journal of Physical Chemistry C*, vol. 114, no. 2, pp. 933–939, 2010.

[8] X. Zhang, Y. Sun, X. Cui, and Z. Jiang, "Carbon-incorporated $TiO_2$ microspheres: facile flame assisted hydrolysis of tetrabutyl orthotitanate and photocatalytic hydrogen production," *International Journal of Hydrogen Energy*, vol. 37, no. 2, pp. 1356–1365, 2012.

[9] Y. Kado, R. Hahn, and P. Schmuki, "Surface modification of $TiO_2$ nanotubes by low temperature thermal treatment in $C_2H_2$ atmosphere," *Journal of Electroanalytical Chemistry*, vol. 662, no. 1, pp. 25–29, 2011.

[10] P. Yang, D. Zhao, D. I. Margolese, B. F. Chmelka, and G. D. Stucky, "Block copolymer templating syntheses of mesoporous metal oxides with large ordering lengths and semicrystalline framework," *Chemistry of Materials*, vol. 11, no. 10, pp. 2813–2826, 1999.

[11] V. G. Hadjiev, M. N. Iliev, and I. V. Vergilov, "The Raman spectra of $Co_3O_4$," *Journal of Physics C: Solid State Physics*, vol. 21, no. 7, pp. L199–L201, 1988.

[12] Y. Teng, L. X. Song, L. B. Wang, and J. Xia, "Face-raised octahedral $Co_3O_4$ nanocrystals and their catalytic activity in the selective oxidation of alcohols," *Journal of Physical Chemistry C*, vol. 118, no. 9, pp. 4767–4773, 2014.

[13] C.-S. Kuo, Y.-H. Tseng, C.-H. Huang, and Y.-Y. Li, "Carbon-containing nano-titania prepared by chemical vapor deposition and its visible-light-responsive photocatalytic activity," *Journal of Molecular Catalysis A: Chemical*, vol. 270, no. 1-2, pp. 93–100, 2007.

[14] W. Ren, Z. Ai, F. Jia, L. Zhang, X. Fan, and Z. Zou, "Low temperature preparation and visible light photocatalytic activity of mesoporous carbon-doped crystalline $TiO_2$," *Applied Catalysis B: Environmental*, vol. 69, no. 3-4, pp. 138–144, 2007.

[15] D. X. Ye, S. Pimanpang, C. Jezewski et al., "Low temperature chemical vapor deposition of Co thin films from $Co_2(CO)_8$," *Thin Solid Films*, vol. 485, no. 1-2, pp. 95–100, 2005.

[16] G. Kwak, J. Hwang, J.-Y. Cheon et al., "Preparation method of $Co_3O_4$ nanoparticles using ordered mesoporous carbons as a template and their application for Fischer-Tropsch synthesis," *The Journal of Physical Chemistry C*, vol. 117, no. 4, pp. 1773–1779, 2013.

[17] T. J. Chuang, C. R. Brundle, and D. W. Rice, "Interpretation of the x-ray photoemission spectra of cobalt oxides and cobalt oxide surfaces," *Surface Science*, vol. 59, no. 2, pp. 413–429, 1976.

[18] J. L. Gautier, E. Rios, M. Gracia, J. F. Marco, and J. R. Gancedo, "Characterisation by X-ray photoelectron spectroscopy of thin $Mn_xCo_{3-x}O_4(1 \geq x \geq 0)$ spinel films prepared by low-temperature spray pyrolysis," *Thin Solid Films*, vol. 311, no. 1-2, pp. 51–57, 1997.

[19] H. Kato and A. Kudo, "Highly efficient decomposition of pure water into $H_2$ and $O_2$ over $NaTaO_3$ photocatalysts," *Catalysis Letters*, vol. 58, no. 2-3, pp. 153–155, 1999.

[20] S. Farhadi, K. Pourzare, and S. Sadeghinejad, "Simple preparation of ferromagnetic $Co_3O_4$ nanoparticles by thermal dissociation of the $[CoII(NH_3)_6](NO_3)_2$ complex at low temperature," *Journal of Nanostructure in Chemistry*, vol. 3, no. 1, pp. 1–7, 2013.

[21] C. Lettmann, K. Hildenbrand, H. Kisch, W. Macyk, and W. F. Maier, "Visible light photodegradation of 4-chlorophenol with a coke-containing titanium dioxide photocatalyst," *Applied Catalysis B: Environmental*, vol. 32, no. 4, pp. 215–227, 2001.

[22] A. Kudo and Y. Miseki, "Heterogeneous photocatalyst materials for water splitting," *Chemical Society Reviews*, vol. 38, no. 1, pp. 253–278, 2009.